Mon. Not. R. Astron. Soc. **322**, L11–L15 (2001)

Chandra detection of the intracluster medium around 3C 294 at $z = 1.786$

A. C. Fabian,* C. S. Crawford, S. Ettori and J. S. Sanders
Institute of Astronomy, Madingley Road, Cambridge CB3 0HA

Accepted 2001 January 25. Received 2001 January 19; in original form 2000 November 30

ABSTRACT

We present a *Chandra* observation of the powerful radio galaxy 3C 294 showing clear evidence for a surrounding intracluster medium. At a redshift of 1.786 this is the most distant cluster of galaxies yet detected in X-rays. The radio core is detected as a point source, which has a spectrum consistent with a heavily absorbed power law, implying an intrinsic 2–10 keV luminosity of $\sim 10^{45}\,\mathrm{erg\,s^{-1}}$. A small excess of emission is associated with the southern radio hotspots. The soft, diffuse emission from the intracluster medium is centred on the radio source. It has an hourglass shape in the north–south direction, extending to radii of at least 100 kpc, well beyond the radio source. The X-ray spectrum of this extended component is fitted by a thermal model with temperature ~5 keV, or by gas cooling from above 7 keV at rates of ~ 400–$700\,\mathrm{M_\odot\,yr^{-1}}$. The rest-frame 0.3–10 keV luminosity of the cluster is $\sim 4.5 \times 10^{44}\,\mathrm{erg\,s^{-1}}$. The existence of such a cluster is consistent with a low-density universe.

Key words: galaxies: active – galaxies: clusters: individual: 3C 294 – intergalactic medium – X-rays: galaxies: clusters – cosmology: observations.

1 INTRODUCTION

Radio galaxies act as luminous beacons which are detectable across the Universe. Powerful radio galaxies at low redshift, such as Cygnus A, lie in rich clusters of galaxies, and it is possible that more distant examples too are in dense environments. They may therefore provide the means to discover the most distant clusters and thus enable the study of cluster evolution. Here we present the detection of luminous diffuse X-ray emission surrounding 3C 294, at redshift $z = 1.786$. This is 40 per cent higher in redshift than previously reported diffuse cluster X-ray emission (Rosati et al. 1999; Stanford et al. 2000).

3C 294 is a very powerful Fanaroff–Riley II (FR II) radio source, associated with an emission-line galaxy. At high resolution the radio structure shows a Z-shaped (double-hotspot) morphology suggestive of precessing jets originating from the weak flat-spectrum core (McCarthy et al. 1990). The galaxy is embedded in a luminous Lyman α halo, elongated to the north and south, and thus roughly aligned with the radio source direction (at position angle 20°). The Lyman α nebula extends over a $\sim 75 \times 125\,\mathrm{kpc}^2$ area (assuming $H_0 = 50\,\mathrm{km\,s^{-1}\,Mpc^{-1}}$ and a cosmological deceleration parameter of $q_0 = 0.5$), and is brighter on the northern side of the source toward the side of the closer and brighter radio hotspot. This side of the nebula has a triangular morphology, such that the radio core is at its southern apex (McCarthy et al. 1990); there is also a hint that the inner part of the southern side of the nebula mirrors this shape. This (bi-)conical morphology is similar to an illumination cone caused by anisotropic radiation from a central ionizing continuum, perhaps arising from dust scattering of radiation from a quasar nucleus. The Lyman α emission shows a large velocity shear of $\sim 1500\,\mathrm{km\,s^{-1}}$ across the whole nebula. The higher ionization lines of C IV $\lambda 1550$, C III] $\lambda 1909$ and He II $\lambda 1640$ are also spatially extended and seem to share this velocity field (McCarthy, Baum & Spinrad 1996).

The northern triangular shape can also be seen on a smaller scale in the K' image of Stockton, Canalizo & Ridgway (1999); there is no obvious extension to the south of the radio core in the near-infrared. The K' image suggests that the apex of the cone may be offset to the north-west from the radio core position by a small amount (~0.2 arcsec). At the redshift of the radio galaxy, the K' emission is expected to be dominated by a stellar population, with little contribution from line emission. The image shows a few resolved knots within the extended continuum, none of which is spatially coincident with any of the radio components.

Benitez, Martinez-Gonzalez & Gonzalez-Serrano (1995) find a slight excess of faint R-band objects within a region of 45-arcsec (~380-kpc) radius around 3C 294, suggestive of the presence of a poor cluster of galaxies around the radio galaxy. The radio source is highly depolarized (Liu & Pooley 1991), indicating a dense surrounding medium.

X-ray emission was detected from the direction of 3C 294 using archival data from the *ROSAT* satellite (Crawford & Fabian 1996). This Position Sensitive Proportional Counter (PSPC) image had too few counts either to resolve any spatial extent or to discriminate between thermal and non-thermal origins for the emission.

---

* E-mail: acf@ast.cam.ac.uk

A subsequent long High Resolution Imager (HRI) exposure showed the source to be very faint, and possibly spatially extended (Hardcastle & Worrall 1999; Dickinson et al 1999). Here we present the first images clearly showing extended diffuse X-ray emission.

2 OBSERVATIONS

3C 294 was observed for 19.5 ks with the *Chandra* X-ray observatory on 2000 October 29 and processed with CXCDS version R4CU5UPD11.1. The telescope (Weisskopf et al. 2000) was pointed such that the target appears 1 arcmin from the centre of chip 7 (S3) in ACIS-S. It is thus 1 arcmin from the nominal aim-point and the on-axis point-spread function applies. The light curve shows no evidence for particle background flares in the detector during the observation, and we have extracted the X-ray data from the total exposure.

2.1 Images

Inspection of the X-ray image shows a number of immediately apparent features (Figs 1 and 2, opposite p. L16). The weak radio core shows up as the brightest X-ray feature, a point source with hard X-ray colours. The outer southern radio hotspot (feature 'H_S' in the McCarthy et al. 1990 map) is spatially coincident with an X-ray excess seen in both hard and soft bands. This excess is only about 2σ above the surrounding diffuse emission. There is a slight hint that there is also excess X-ray emission at the positions of the inner hotspot and lobe ('K_S' and 'L_S') on this side (Fig. 1). We find no evidence for any X-ray emission associated with the hotspots to the northern side of the radio source. Curiously, though, there is an X-ray point source at $\mathrm{RA} = 14^{\mathrm{h}}06^{\mathrm{m}}44\overset{\mathrm{s}}{.}810$, $\mathrm{Dec.} = +34°11'35\overset{''}{.}74$ (J2000) that continues the line of the radio source axis on this side. At a distance of ~15 arcsec from the core, the source is too far away to be associated with any known radio components. It is probably a serendipitous background source or even another active galaxy within the cluster, but we find no evidence for a counterpart in the Digitized Sky Survey or any archival optical images of this field.

The bright X-ray source associated with the radio core clearly lies at the centre of a soft and spatially extended component of X-ray emission (Fig. 2). This very extended component shares and extends the biconical structure of the Lyman α nebula (Fig. 3): a triangular shape to the north, with an opening angle of around 80°, and one to the south with a slightly larger opening angle, both with the radio core at an apex. The total extended shape resembles an hourglass.

The two sides of the structure are much more evenly matched in flux than is seen in the Lyman α or near-infrared. If anything, the southern side is slightly brighter, particularly close in to the radio core, whereas the northern side appears to have a slight deficit in the cone near to the core (Fig. 1). We cannot, however, rule out the possibility that the inner radio hotspot and lobe contribute some of this excess brightness close to the core in the southern cone. The soft component extends out to radii of ~13 arcsec (just over 100 kpc) to both the north and south, almost twice as far as the extent of the radio source structure.

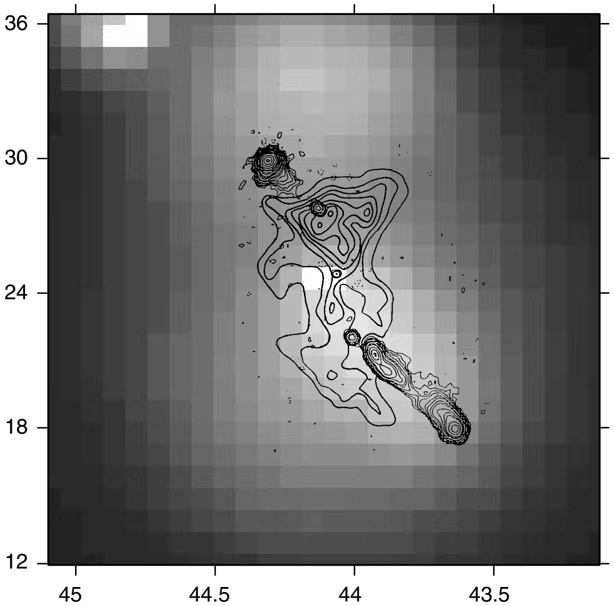

Figure 3. Grey-scale smoothed image of *Chandra* emission from 3C 294 (Fig. 1), with the radio (tightly bunched contours) and Lyman α (more open contours) emission superposed (taken from McCarthy et al. 1990).

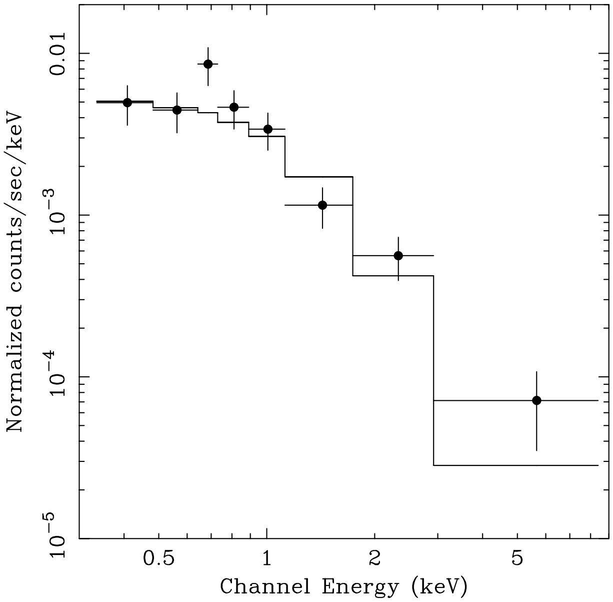

Figure 4. Spectrum of the soft extended component of the X-ray emission (solid circles), with the best-fitting isothermal model of temperature 4.9 keV.

2.2 Spectra

We extracted the spectrum of the soft extended emission in both the northern and southern cones, excluding a small region encompassing the central bright core and the bright source ~15 arcsec to the north-west. The data have been grouped into bins with a minimum of 15 counts. We fitted the spectrum with a thermal MEKAL model, although with only about 110 counts from the source we are not able to place strong constraints on the emission properties. We assume that the extended emission is at the redshift of the radio galaxy, and that there is no absorption in excess of the line-of-sight Galactic hydrogen column of $1.2 \times 10^{20}\,\mathrm{cm}^{-2}$, and freeze the abundance to be $0.3 \times$ solar. The best fit (reduced χ^2 of 1.58 for six degrees of freedom) yields a temperature for an isothermal spectrum of $kT_{\mathrm{X}} = 5.0^{+2.6}_{-1.5}$ keV (Fig. 4; errors are 1σ). With 90 per cent confidence the temperature exceeds 2.9 keV. The intrinsic (i.e. corrected for Galactic absorption) 0.3–10 keV (rest-frame) luminosity is $4.5 \times 10^{44}\,\mathrm{erg\,s^{-1}}$; the 2–10 keV luminosity is $(2.5 \pm 0.4) \times 10^{44}\,\mathrm{erg\,s^{-1}}$. Alternatively, if we fit the extended X-ray emission by a cooling plasma (Johnstone et al. 1992) at an abundance of 0.4×solar (Allen & Fabian 1998), the best fit (reduced χ^2 of 1.44 for six degrees of freedom) gives a gas cooling rate of 400–700 $\mathrm{M_{\odot}\,yr^{-1}}$ from a temperature of >15 to 8 keV, respectively. The 90 per cent lower limit on the cooling flow temperature is 7 keV. We repeated the spectral fitting of the extended emission now excluding the region around the south-western hotspot, and found that the results do not differ significantly. The spectrum is also consistent with power-law emission (photon index of 1.96 ± 0.35).

We also examined the spectrum of the point X-ray source associated with the radio core, but with ~30 counts we can only obtain approximate properties. Most of the counts from this source are only above 2 keV; from modelling the spectrum with a power-law model of photon index $\Gamma = 2$, this implies an excess absorption (i.e. over the Galactic column) of $\sim 7 \pm 3 \times 10^{23}\,\mathrm{cm^{-2}}$. The total (de-absorbed) 2–10 keV (rest-frame) luminosity of the nucleus is then $\sim 1.1 \times 10^{45}\,\mathrm{erg\,s^{-1}}$. Both the intrinsic luminosity and the line-of-sight absorption to the central powerhouse make it comparable to the central source of Cygnus A (Ueno et al. 1994), and steep-spectrum radio quasars in general.

3 DISCUSSION

3.1 Inverse Compton emission?

The stronger low-redshift powerful 3C galaxies, such as Cygnus A (Wilson, Young & Shopbell 2000) and 3C 295 (Harris et al. 2000), show soft X-ray emission associated with the position of the outer radio lobes. This is interpreted as being due to inverse Compton (IC) scattering of cosmic microwave background photons by the relativistic electrons in the radio plasma. The energy density of the microwave background is 60 times higher at $z = 1.786$ than at the current epoch, so the cooling time of relativistic electrons is short. It has also been predicted that these electrons can also IC-scatter photons from the nucleus, to produce an asymmetric, but spatially extended, component of X-ray emission (e.g. Brunetti, Setti & Comastri 1997). In this scenario the X-ray emission arising in the more distant radio lobe is expected to be brighter owing to the stronger back-scattering of photons towards the observer. We do find tentative X-ray emission associated with the southern outer hotspot, and also possibly with the inner hotspot and lobe to this side. There is no obvious excess of emission associated with the northern radio source components. Assuming that the southern side is the further lobe, then the observed excess may fit predictions.

The lack of any clear correspondence of X-ray emission with the northern radio hotspot, or of any widespread diffuse radio emission, and the extension of the diffuse X-ray emission beyond the radio source, indicates that IC scattering by an electron population related to the radio emission contributes only a small fraction of the total X-ray luminosity observed with *Chandra.*

The possibility remains that the emission is due to an older population of relativistic electrons IC scattering the microwave background (see e.g. Sarazin 1999). The required Lorentz factor is then about 300 and the cooling time of the electrons $t_{\mathrm{ic}} = 5 \times 10^7$ yr. Can such emission mimic hot cluster gas? We note that (i) to distribute electrons to 100-kpc radius requires supersonic motion, and (ii) to confine them requires a substantial atmosphere of gas with a pressure exceeding that of the relativistic gas (or it would explode outward). Assuming that the gas pressure required is at least a times the minimum inferred from the observed X-rays (i.e. $aL_{\mathrm{X}}t_{\mathrm{ic}}/V$, where V is the volume within 100 kpc; a must include electron, proton and magnetic pressures), then we find that the predicted X-ray luminosity of the atmosphere, if $kT_{\mathrm{X}} = 1$ keV, equals that seen below 1 keV if $a = 10$. In other words, to confine a fossil electron population in a gravitational well shallower than implied by a thermal interpretation of the X-ray spectrum overpredicts the observed soft X-ray flux, unless the thermal overpressure $a < 10$.

3.2 An intracluster medium

The spatial scale of the extended soft X-ray component is comparable to that expected from the inner parts of an intracluster medium centred on 3C 294, particularly if there is a cooling flow in the cluster (Fabian 1994). This interpretation is supported by its spectrum; the relatively high temperature of the gas, $kT > 2.9$ keV, indicates that we are dealing with a cluster, and not just the hot halo of a massive galaxy. The 0.3–2 keV luminosity that we find for the extended component from the *Chandra* data ($\sim 2 \times 10^{44}\,\mathrm{erg\,s^{-1}}$) is in good agreement with the 0.7–2 keV luminosity of $1.7 \times 10^{44}\,\mathrm{erg\,s^{-1}}$ that we inferred from the *ROSAT* PSPC data. The *Chandra* data confirm that any nuclear X-ray emission is strongly absorbed below 2 keV, and thus could not have made a major contribution to the observed *ROSAT* flux from 3C 294. We thus confirm our original supposition that the *ROSAT* X-ray emission associated with this source was from a surrounding cluster of galaxies (Crawford & Fabian 1996; see also Hardcastle & Worrall 1999; Dickinson et al. 1999). The X-ray luminosity observed suggests that 3C 294 is embedded in only a relatively modest cluster, although at this large a distance we are probably only seeing the central regions of a cluster with a cooling flow. The cluster has about half the luminosity of the cluster surrounding the powerful low-redshift FR II radio source Cygnus A. It also fits the temperature–luminosity function for nearby clusters (Fig. 5).

The asymmetric hourglass structure of the diffuse X-ray emission is different from that generally seen in low-redshift clusters. The X-ray data raise the intriguing possibility that the triangular shapes observed in the Lyman α and K' images are *not* due to an illumination cone prescribed by the opening angle for escaping quasar radiation, but instead arise from the physical distribution of the gas around the source. If this is the case, it is curious that the regions apparently deficient in X-ray gas are *not* associated with the radio source direction, in contradiction to the X-ray cavities seen in *Chandra* images of clusters around nearby radio sources (Fabian et al. 2000; McNamara et al. 2000). If the inner hotspot describes the current pointing position of the radio jets, they seem to be directed almost into the densest extended X-ray emission. If the radio outflow was oriented more east–west at a much earlier stage of the central source (consistent with the direction of the jet precession), it may well have shaped the X-ray gas. Of course, such cavities need not be devoid of gas, since the medium may be multiphase and the brighter parts may just be those where the cooler gas is most abundant.

A peaked, bright X-ray core to a cluster is characteristic of a

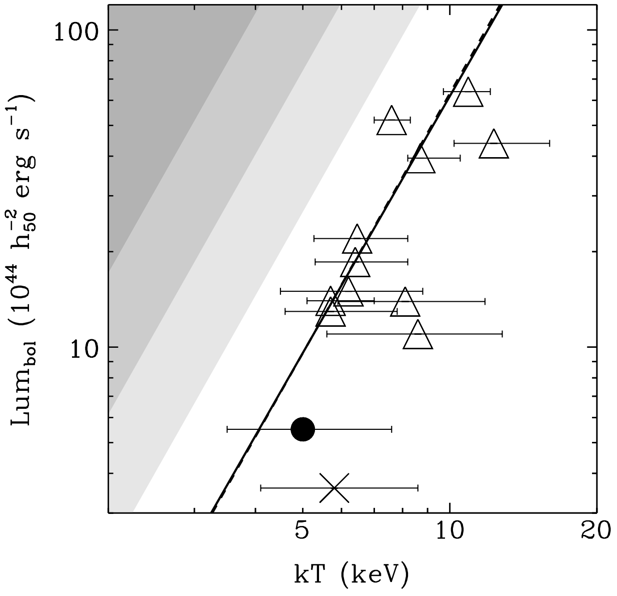

Figure 5. Luminosity–temperature relation for galaxy clusters with $z > 0.5$ (EMSS: Donahue et al. 1999; RDCS:Della Ceca et al. 2000; Schindler 1999). The dot represents 3C 294, and the cross represents the RCDS cluster RX J0949+4452 at $z = 1.26$ (Stanford et al. 2000). The solid line is the best fit for data of a sample of galaxy clusters with temperature and luminosity corrected by the presence of cooling flows (Ettori, Allen & Fabian 2001). The dashed line is the best fit for nearby clusters from Wu, Xue & Fang (1999). The shaded region on the left shows the expected shift of the *L–T* relation for evolution with $1 < A < 2$, $2 < A < 3$ and $A > 3$ (darker shades respectively) at $z = 1.786$ using the relation $L \sim T^s(1+z)^A$. As shown by Borgani et al. (1999) for the RCDS, $\Omega_0 = 1$ models require positive evolution of the *L–T* relation (i.e. $1 < A < 3$), whereas no evolution implies low-Ω_0 cosmologies.

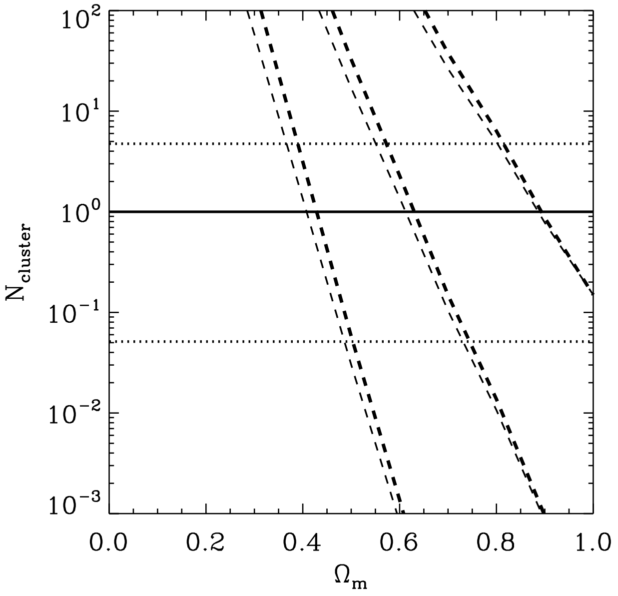

Figure 6. *Maximum* number of collapsed objects beyond redshift 1.786 with virial mass larger than that corresponding to 3, 5 and 9 keV (from right to left). The dashed lines are for $\Omega_m + \Omega_\Lambda = 1$ (thick) and $\Omega_\Lambda = 0$ (thin). Ω_Λ is the contribution to Ω_0 from the cosmological constant. The single detection puts an upper limit on Ω_m. The horizontal lines represent 90 per cent uncertainties on a single detection (Gehrels 1986).

cooling flow, such as are seen around powerful radio galaxies such as Cygnus A (Reynolds & Fabian 1996) and 3C 295 (Allen et al 2001). Extended Lyman α emission is also seen from the nebulosities in low-redshift cooling flows (Fabian, Nulsen & Arnaud 1984; Hu 1992), although the Lyman α luminosity of 3C 294 is very high (and comparable to the X-ray luminosity). The existence of a cooling flow in the 3C 294 cluster is plausible, since the mean density of the gas within 100 kpc of the radio source is 0.02 cm^{-3} and the mean cooling time is about 2 Gyr, less than the age of the Universe at that epoch (3 Gyr, for the adopted cosmology). The pressure of the intracluster medium is consistent with the pressure determined from equipartition arguments for the low surface brightness radio emission around the southern radio emission by McCarthy et al. (1990). Strong Faraday rotation is also observed for the radio source (Liu & Pooley 1991), a further characteristic of cooling flows (Taylor, Barton & Ge 1994). Our results reinforce our earlier hypothesis that powerful radio galaxies may be a way to discover distant cooling flows (Fabian et al. 1986).

As a final consideration of the surrounding gas, we have estimated whether electron scattering of nuclear X-ray emission could contribute significantly to the observed flux (and thus the inferred temperature). Given the parameters of the gas and the central source, the Thomson depth is 0.004 and the scattered flux (assuming that half of the sky is obscured at the nucleus) is only about 1 per cent of the observed flux. If instead the flux detected from the nucleus is also scattered, so that the nucleus is really much more luminous, then we require its 2–10 keV luminosity to be about 2 orders of magnitude greater. (The Thomson depth hardly changes if we reduce the gas temperature to 1 keV and find the densest cluster consistent with the spectrum.) Its bolometric luminosity is then $\sim 5 \times 10^{48}$ erg s^{-1}, assuming that the spectral energy distribution follows that for quasars found by Elvis et al. (1994). Much of this should be absorbed and reradiated in the far-infrared. It is ruled out by 60- and 100-μm limits from *IRAS*, which are about an order of magnitude smaller (1σ levels of 28 and 111 mJy at 60 and 100 μm respectively have been obtained using the web-based XSCANPI at IPAC). We conclude that scattered X-ray emission is unimportant.

3.3 The occurrence of such high-redshift clusters

Following the calculation of Donahue et al. (1998) for the cluster MS 1054-0321, we now estimate how rare a cluster resembling that around 3C 294 might be at this redshift. For simplicity we first adopt an $\Omega_0 = 1$ universe, and use the results from our MEKAL spectral fit, with a conservative lower limit to the temperature of the intracluster medium of 3 keV. The temperature of an equivalent cluster at $z = 0$ is thus $kT_X > 1$ keV [$T_X \propto (1+z)$ for $\Omega_0 = 1$], and its virial mass is greater than $1.3 \times 10^{14}\,\mathrm{M}_\odot$ (Henry 2000). We extrapolate the temperature function of Henry (1997) to estimate that the present-day number density of clusters hotter than 1 keV is less than $2.4 \times 10^{-5}\,\mathrm{Mpc}^{-3}$. Thus the mean virialized mass density in such clusters is less than $3.3 \times 10^9\,\mathrm{M}_\odot\,\mathrm{Mpc}^{-3}$. The assumption of Gaussian perturbations in an $\Omega_0 = 1$ universe allows us to use the integral form of the Press–Schechter (1974) formula to derive the comoving mass density of virialized objects with virial masses greater than M from the current matter density, ρ_0; here, ν_c is the critical threshold at which the perturbations leading to these structures arise. For a present-day cluster with $kT_X > 1$ keV, $\nu_c > 2.0$. As $\nu_c \propto (1+z)$ for a fixed mass scale, this implies that $\nu_c > 5.6$ for similar clusters at

$z = 1.786$ (i.e. $kT_X > 3$ keV then). Using the Press–Schechter formula to obtain the comoving virialized density of such systems as a function of redshift, we integrate the result for $z > 1.786$, assuming the area of the 3C catalogue (north of $\delta = -5°$), to obtain the predicted total number of clusters (see Fig. 6, which also shows results for other values of the matter density parameter Ω_m). The detection of a $kT_X > 3$ keV cluster at $z = 1.786$ is inconsistent with $\Omega_m = 1$.

4 CONCLUSIONS

The *Chandra* observation of 3C 294 reveals soft, spatially extended, X-ray emission that is clearly resolved from any X-ray emission associated with the radio source components. We detect a possible excess of X-ray emission at the site of the southern radio hotspots. The diffuse X-ray emission has an unusual hourglass morphology that is roughly aligned near the centre with the extended Lyman α and K' emission associated with the radio galaxy. The soft extended component is centred on the active nucleus, and with a diameter of over 200 kpc is on a larger scale than that of the embedded radio source. Its X-ray spectrum is fitted well by a thermal model with a temperature of at least 3 keV, and we identify it as the intracluster medium around 3C 294. At $z = 1.786$, this is the first X-ray detection of a cluster of galaxies above $z = 1.3$. Its temperature and the lack of evolution in the L_X–T_X relation out to this redshift both support $\Omega_m < 1$.

Further, much deeper, observations with *Chandra* will enable both the radio and diffuse hot gas components to be better studied. Of great interest for the latter are the temperature and density structure of the intracluster medium, as well as its metallicity. Ω_m can also be constrained from the observed temperature.

ACKNOWLEDGMENTS

We are grateful to NASA and the *Chandra* project for the superb X-ray data, and thank Steve Allen for discussions. ACF and CSC thank the Royal Society for financial support.

REFERENCES

Allen S. W. et al., 2001, MNRAS, submitted
Allen S. W., Fabian A. C., 1998, MNRAS, 297, L63
Benitez N., Martinez-Gonzalez E., Gonzalez-Serrano J. K., 1995, AJ, 109, 935
Borgani S., Rosati P., Tozzi P., Norman C., 1999, ApJ, 517, 40
Brunetti G., Setti G., Comastri A., 1997, A&A, 325, 898
Crawford C. S., Fabian A. C., 1996, MNRAS, 282, 1483
Della Ceca R., Scaramella R., Gioia I. M., Rosati P., Fiore F., Squires G., 2000, A&A, 353, 498
Dickinson M., Mushotzky R. F., Spinrad H., McCarthy P. J., van Breugel W. J. M., 1999, ApJ, submitted
Donahue M., Voit G. M., Gioia I., Luppino G., Hughes J. P., Stocke J. T., 1998, ApJ, 502, 550
Donahue M., Voit G. M., Scharf C. A., Gioia I. M., Mullis C. R., Hughes J. P., Stocke J. T., 1999, ApJ, 527, 525
Elvis M. J. et al., 1994, ApJS, 95, 1
Ettori S., Allen S. W., Fabian A. C., 2001, MNRAS, 322, 187
Fabian A. C., 1994, ARA&A, 32, 277
Fabian A. C., Nulsen P. E. J., Arnaud K. A., 1984, MNRAS, 208, 179
Fabian A. C., Arnaud K. A., Nulsen P. E. J., Mushotzky R. F., 1986, ApJ, 305, 9
Fabian A. C. et al., 2000, MNRAS, 318, L65
Gehrels N., 1986, ApJ, 303, 336
Hardcastle M., Worrall D. M., 1999, MNRAS, 309, 969
Harris D. E. et al., 2000, ApJ, 530, L81
Henry J. P., 1997, ApJ, 489, L1
Henry J. P., 2000, ApJ, 534, 565
Hu E. M., 1992, ApJ, 391, 608
Johnstone R. M., Fabian A. C., Edge A. C., Thomas P. A., 1992, MNRAS, 255, 431
Liu R., Pooley G., 1991, MNRAS, 249, 343
McCarthy P. J., Spinrad H., van Breugel W. J. M., Liebert J., Dickinson M., Djorgovski S., Eisenhardt P., 1990, ApJ, 365, 487
McCarthy P. J., Baum S. A., Spinrad H., 1996, ApJS, 106, 281
McNamara B. R. et al., 2000, ApJ, 534, L135
Press W., Schechter P., 1974, ApJ, 187, 425
Reynolds C. S., Fabian A. C., 1996, MNRAS, 278, 479
Rosati P., Stanford S. A., Eisenhardt P. R., Elston R., Spinrad H., Stern D., Dey A., 1999, AJ, 118, 76
Sarazin C. L., 1999, ApJ, 520, 529
Schindler S., 1999, A&A, 349, 435
Stanford S. A., Holden B., Rosati P., Tozzi P., Borgani S., Eisenhardt P. R., Spinrad H., 2000, ApJ, submitted (astro-ph/0012250)
Stockton A., Canalizo G., Ridgway S. E., 1999, ApJ, 519, L131
Taylor G. B., Barton E. L., Ge J.-P., 1994, AJ, 107, 1942
Ueno S., Koyama K., Nishida M., Yamauchi S., Ward M. J., 1994, ApJ, 431, L1
Weisskopf M. C., Tanabuam H. D., Van Spebroeck L. P., O'Dell S. L., 2000, Proc. SPIE, 4012, in press (astro/ph-0004127)
Wilson A. S., Young A. J., Shopbell P. L., 2000, ApJ, 544, 27
Wu X.-P., Xue Y.-J., Fang L.-Z., 1999, ApJ, 524, 22

This paper has been typeset from a TEX/LATEX file prepared by the author.

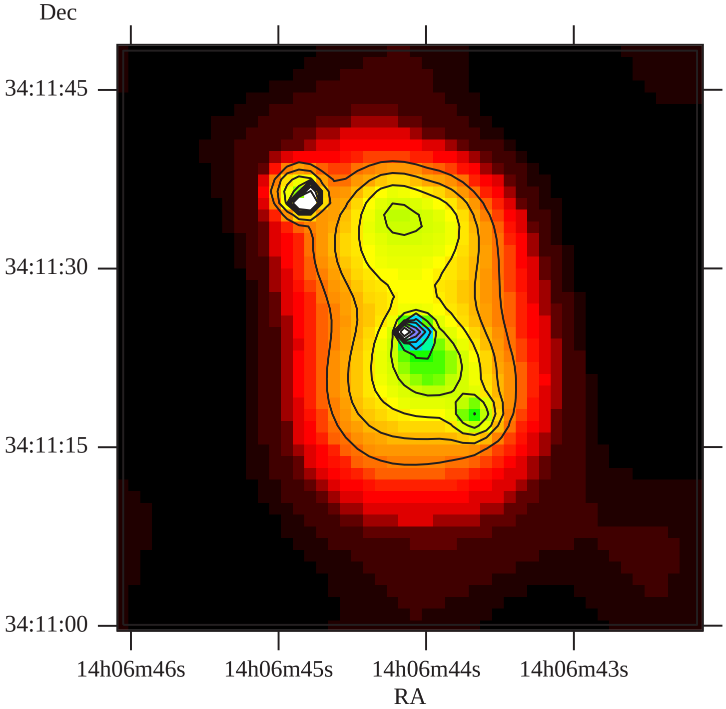

Figure 1. Adaptively smoothed image and contours of the 0.5–5 keV *Chandra* emission from 3C 294. The significance level for smoothing is set at 2σ. Contours shown start at 0.048 count arcsec^{-2}, doubling at each level. 1 arcsec corresponds to 8.4 kpc for the assumed cosmology.

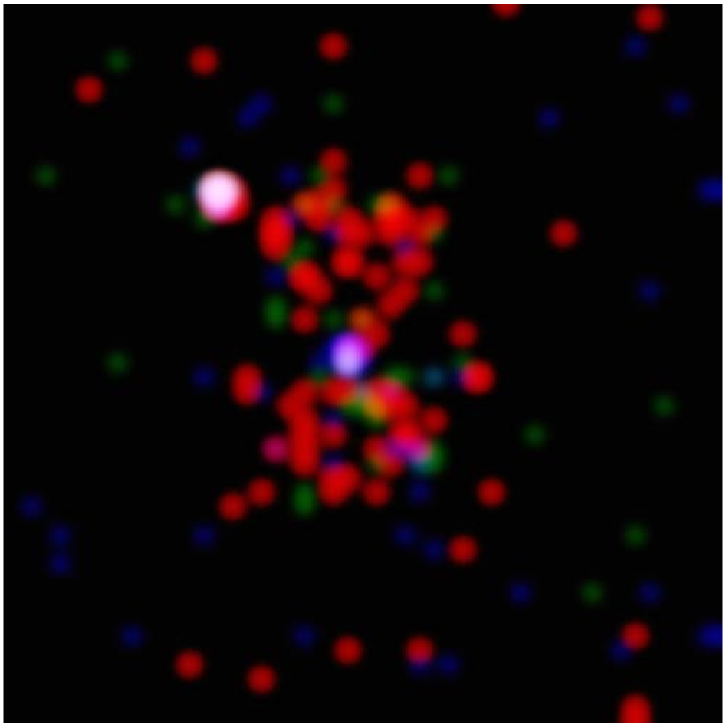

Figure 2. X-ray colour map of the *Chandra* emission from 3C 294: 0.5–1 keV is shown as red, 1–2 keV as green, and 2–5 keV as blue. The data have been binned by 2 pixels (i.e. 1 arcsec), and smoothed by 2 pixels. North is to the top and east to the left, and the image is approximately 1.2 arcmin on a side.